UDK 546.62:623.522
Original scientific article/Izvirni znanstveni članek

ISSN 1580-2949
Mater. Tehnol.

EXPERIMENTAL STUDY ON BALLISTIC PERFORMANCE OF FUNCTIONALLY GRADED COMPOSITES REINFORCED WITH TiB_2

EKSPERIMENTALNA ŠTUDIJA BALISTIČNIH LASTNOSTI FUNKCIONALNO GRADIRANIH KOMPOZITOV OJAČANIH S TiB_2

[1]Muhammed Soner Başer, [2]Ömer Faruk Demírok, [3]Ömer Savaş

[1]Republic of Turkey Presidential Complex, Department of State Information Coordination Center, 06560 Bestepe, Ankara, Turkey
[2]Sakarya University of Applied Sciences, Maritime Higher Vocational School, 54800 Sakarya, Turkey
[3]Yıldız Technical University, Faculty of Naval Architecture and Maritime, Department of Marine Engineering, 34353 Istanbul, Turkey

Prejem rokopisa – received: 2026-01-12; sprejem za objavo – accepted for publication: 2026-06-18

doi:10.17222/mit.2026.1645

This study investigates the fabrication of pure Al and Al–4%Cu ingots containing functionally graded layers (FGL) reinforced with in-situ synthesized TiB2 particles by gravitational casting, and the experimental evaluation of their ballistic performance. Ingots with varying FGL thicknesses were produced using the sedimentation technique, and their physical properties (microstructure, phase analysis, density, reinforcement volume fraction, elasticity) as well as ballistic performance were assessed through depth of penetration (DOP) tests. Al-based ingots with (5, 10 and 15) mm FGL, Al–Cu ingots with 10 mm FGL, and non-FGL Al–Cu ingots were successfully fabricated. Results demonstrate that ballistic efficiency increases proportionally with FGL thickness, with optimum performance observed in the 10–15 mm range, while the differential efficiency factor (DEF) decreases beyond 15 mm. Furthermore, an addition of 4 % Cu to the matrix alloy enhanced ballistic performance by 37.5 % compared to the 10 mm FGL sample without Cu, underscoring the critical role of the Cu addition in improving ballistic protection.

Keywords: functionally graded layer (FGL), ballistic simulation, depth of penetration (DOP) test

V članku avtorji predstavljajo študijo, ki obravnava izdelavo ingotov iz čistega aluminija (Al) in zlitine Al s 4 % Cu s funkcionalno gradientnimi plastmi (FGL, angl.: functionally graded layers), ojačanimi z delci TiB_2, *in-situ* sintetiziranimi s postopkom gravitacijskega litja. Po izdelavi je sledilo eksperimentalno ovrednotenje njihove balistične zmogljivosti. S tehniko sedimentacije so avtorji izdelali ingote z različnimi debelinami FGL, določili mikrostrukturo, izvedli fazno analizo ter določili gostoto, volumski delež ojačitve in elastičnost. Balistično zmogljivost pa so ocenili s preizkusi globine penetracije (DOP; angl: Depth of Penetration). Avtorji so uspešno izdelali ingote na osnovi Al s plastmi FGL debeline (5, 10 in 15) mm, ingote iz zlitine Al–Cu s plastjo FGL debeline 10 mm ter ingote iz zlitine Al–Cu brez plasti FGL. Rezultati raziskave so pokazali, da se balistična učinkovitost povečuje sorazmerno z debelino FGL, pri čemer je bila optimalna zmogljivost zabeležena v območju med 10 in 15 mm, medtem ko se je faktor diferencialne učinkovitosti (DEF; angl.: Differential Efficiency Factor) pri debelinah nad 15 mm zmanjšal. Poleg tega je dodatek 4 % Cu osnovni kovini izboljšal balistično zmogljivost za 37,5 % v primerjavi z vzorcem z 10 mm debelo plastjo FGL brez Cu, kar poudarja ključno vlogo dodatka Cu pri izboljšanju balistične zaščite.

Ključne besede: funkcionalna gradientna plast, balistična simulacija, preizkus globine penetracije

1 INTRODUCTION

Functionally graded materials (FGMs) are increasingly utilized in armor technologies due to their ability to optimize material properties through gradual variations in constituent volume fractions.[1] These materials integrate distinct properties of ceramics and metals, where the hard outer layer effectively blunts and erodes projectiles, while the soft inner layer absorbs kinetic energy upon impact.[2] Moreover, the smooth transition between adjacent components attenuates stress reflection waves, thus delaying structural failure.[3] This unique combination enables FGMs to offer enhanced ballistic resistance and structural integrity, making them promising candidates for armor applications in extreme environments requiring high impact resistance and superior ballistic performance.

In armor systems, aluminum metal matrix composites reinforced with intermetallic and ceramic particles such as Al_3Ti, B_4C, SiC, and TiB_2 are commonly used due to their grain-refining characteristics.[4] The high strength, high wear resistance and low density of TiB_2 particles make it a popular choice for improving the performance and durability of metal matrix composites.[1] In addition, TiB_2 does not react with the aluminum matrix; it remains thermodynamically stable within aluminum and also acts as a nucleation agent for aluminum, thereby promoting grain refinement.[5] The mechanical and tribological properties of aluminum matrix composites (AMCs) are significantly influenced by grain refinement in the matrix.[6,7]

TiB_2, as a ceramic, is a good choice as an armor material as it offers most properties required for an armor material such as high hardness, compressive strength,

*Corresponding author's e-mail:
muhammedsonerbaser@gmail.com (Muhammed Soner Başer)

© 2026 The Author(s). Except when otherwise noted, articles in this journal are published under the terms and conditions of the Creative Commons Attribution 4.0 International License (CC BY 4.0).

elastic modulus and ballistic efficiency.[8] Pettersson et al.[9] demonstrated that Ti-TiB_2 FGMs formed via spark plasma sintering exhibited superior ballistic resistance compared to pure TiB_2. Balcı et al.[10] investigated three-layer B_4C/AA7075 FGMs produced by hot pressing, finding their performance against 7.62 mm armor-piercing (AP) rounds inferior to Al_2O_3/Al laminated composites and Al_2O_3/4340 steel. Similarly, Ubeyli et al.[11] reported that SiC/7075Al FGMs with varying volume fractions did not show improved resistance to 7.62 mm AP impacts. DOP testing, introduced by Rozenberg et al. in the 1980s, has become a standard method, measuring projectile penetration into support material with and without ceramic tiles to assess their effectiveness.[12,13]

The methods used for the fabrication of Al–TiB2 metal matrix composites (MMCs) are generally classified into solid–liquid and solid–solid reaction processes. In addition, these fabrication routes can be categorized as ex situ and in situ techniques.[14] The ex situ method involves the incorporation of pre-synthesized reinforcement particles into the molten aluminum; however, it suffers from several limitations, such as non-uniform particle distribution, weak interfacial bonding, and thermodynamic instability.[15] In contrast, the in situ approach allows the reinforcement phases to be formed directly within the matrix, providing significant advantages such as uniform particle distribution, effective grain refinement, clean and well-bonded interfaces, superior thermal stability, and a more economical processing route.[16,17]

In this study, the production, characterization and ballistic performance of Al-220 and Al-4%Cu based ingots containing TiB_2 reinforced functional graded layer by sedimentation method[18,19] were investigated. Sedimentation is a removal mechanism that takes advantage of the density difference between the molten metal and inclusions.[20] Particles with a higher density than the melt tend to settle toward the bottom; however, the settling rate is also influenced by the morphology of the particles. TiB_2 particles were synthesized in situ at an appropriate temperature according to the corresponding phase diagram, followed by a slow cooling process. At low cooling rates, the volume fraction of intermetallic phases increases and the particle size becomes larger. When the melt is maintained for an extended period just above the liquidus temperature, intermetallic compounds grow as primary phases and settle to the bottom due to the density difference.[21] The study includes in-situ synthesis of TiB_2 particles, sedimentation of these particles and the effects of layer thicknesses on ballistic performance by creating different layer thicknesses. In addition, the effect of the addition of 4 % Cu in the pure Al-based ingot on ballistic performance efficiency was observed. DOP test method will be used to evaluate the ballistic performance effects.

2 EXPERIMENTAL STUDIES

2.1 Production and characterization of composites

In the study, the production of ingots was carried out in 2 stages: synthesizing TiB_2 particles and creation of functional graded layer by precipitating TiB_2 particles.

2.2 Synthesizing TiB_2 particles

In this study, Al-10Ti and Al-3B master alloys were used as Ti and B sources for TiB_2 formation. The aim of the study is to synthesize TiB_2 enhancer particles by in-situ technique. Instead of this technique, liquid Al-Ti-B solution is firstly prepared, followed by the synthesis of TiB_2 particles by applying cooling process.

According to the Al-B and Al-Ti phase diagrams, Ti and B are present in the master alloys in the form of Al_3Ti, AlB_{12} and AlB_2 compounds and the solubility of boron in aluminum is quite low (about 1.5 % at 1200 °C).[22] In order for all of the Ti and B in solution to be converted into TiB_2, the Ti:B ratio by weight should be 2.15.

2.3 Creation of Functional Graded Layers

In this study, melting and solidification parameters were optimized by adjusting temperature and holding time to achieve the desired Functionally Graded Layer (FGL) formation. Alloy solutions, prepared according to **Table 1**, were first held at 1200 °C for 1 h in a resistance melting furnace to obtain the Al-Ti-B solution, then cooled to 750 °C and maintained for 2 h to facilitate the in-situ synthesis of TiB_2 particles, which precipitated and settled at the bottom of the melt. These optimized conditions resulted in ingots with FGL thicknesses of 0.5 cm, 1 cm, and 1.5 cm, which were subsequently allowed to cool gradually within the furnace.

The ingots were melted and solidified in 5 mm thick ceramic molds, designed in a conical shape (**Figure 1a**) to ensure non-porous formation, while **Figures 1b–1d** il-

Table 1: TiB_2 Reinforcement Thicknesses After Sedimentation

Specimen code	Targeted FGL thickness, mm	mTi (g)	mB (g)	mCu (g)	mAl (g)	$mTiB_2$ (g)	mTOTAL (g)
5 mm-FGL-Al ingot	5	10.30	4.66	0	991.04	14.96	1006
10 mm-FGL-Al ingot	10	20.60	9.32	0	972.08	29.92	1002
15 mm-FGL-Al ingot	15	30.9	13.98	0	963.12	44.88	1008
10 mm-FGL-(Al-Cu) ingot	10	20.60	9.32	60	1032.08	29.92	1060
Non-FGL-(Al-Cu) ingot	0	0	0	60	968	0	1032

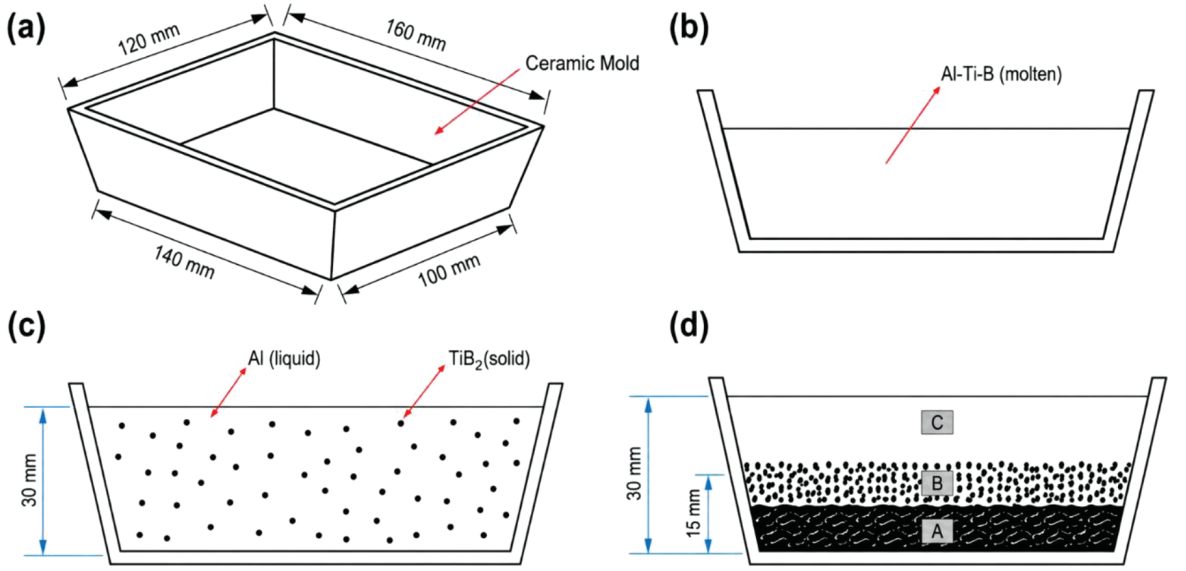

Figure 1: a) ceramic mold image and its dimensions, b) Al-Cu-Ti-B solution at 1200 C, c) Synthesis of TiB_2 particles in liquid matrix by in-situ method at 800 C, d) functional grading (A-B-C regions) TiB_2 particles with the effect of gravity after waiting for 2 h at 800 C

lustrate the Al-Ti-B solution formation, TiB_2 particle synthesis, and the obtained FGLs, respectively.

For the characterization of the prepared ingots, A-B and C regions were identified. The FGL layers were labeled A and B and the unreinforced pure Al or Al-Cu regions without TiB_2 were labeled C. Layers A and B were determined by dividing the reinforcement thicknesses into two equal parts. The main reason for dividing the FGLs into 2 separate layers for characterization is to observe the functional grading. The reason why the unreinforced layers alone are named as zone C is that they have homogeneous properties since they are not reinforced and there are no major changes in their mechanical properties.

2.4 Ballistic Test

The ingots were machined to dimensions of 60 × 75 × 25 mm using a CNC milling machine for ballistic testing, as shown in **Figure 2**. **Figures 2a–2b** present the Al-Cu ingots without and with a 10 mm Functionally

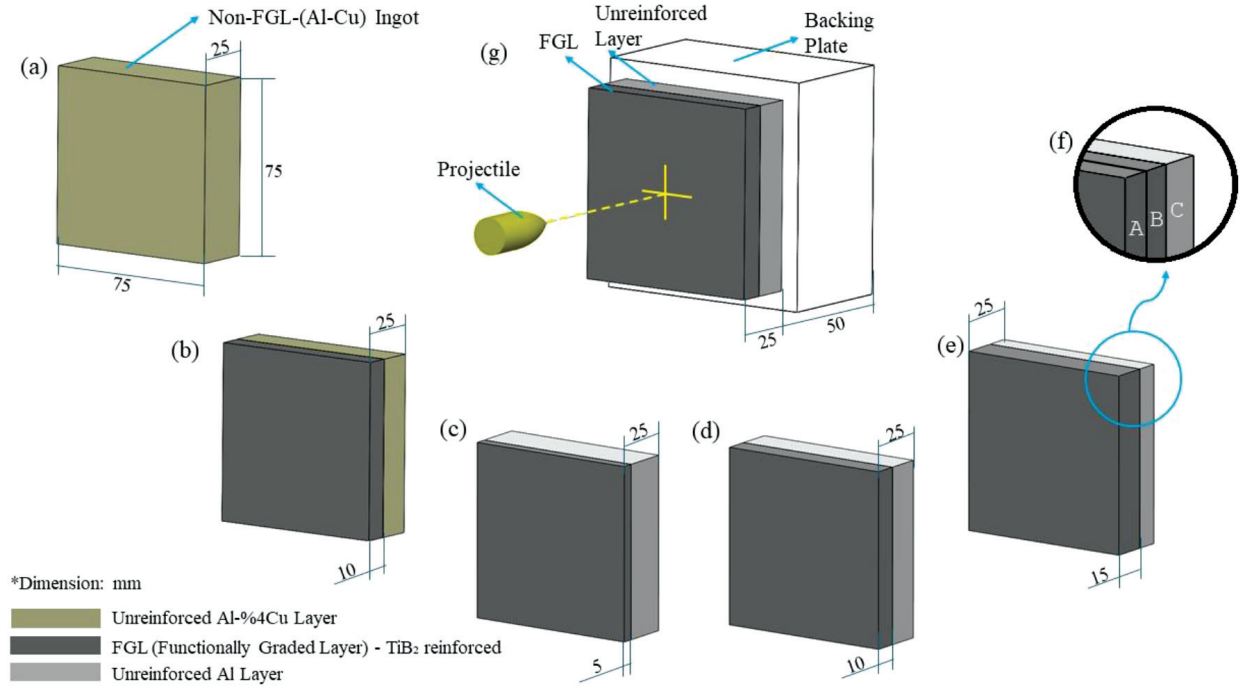

Figure 2: Producted FGL and DOP Test: a) Non-FGL – (Al-Cu) Ingot, b) Non-FGL – (Al-Cu) Ingot, c) 5 mm FGL – Al Ingot, d) 10 mm FGL – Al Ingot, e) 15 mm FGL – Al Ingot, f) Designated Composite Layers for Characterization and g) DOP Test Configuration

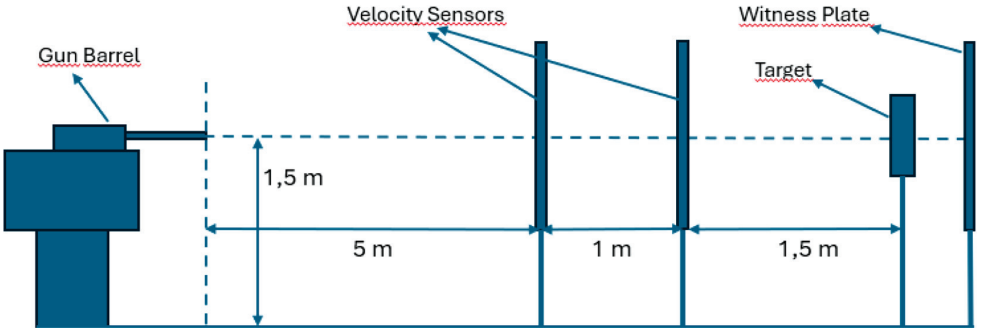

Figure 3: Schematic Diagram of Experimental Setup

Graded Layer (FGL), respectively, while **Figures 2c–2e** show Al ingots containing FGLs of 5 mm, 10 mm, and 15 mm thicknesses. To illustrate the functional gradation, the FGL was divided into two regions (A and B), and the unreinforced zone was designated as region C, as indicated in **Figure 2f**.

Ballistic tests were carried out in a specialized ballistic test laboratory certified to international standard. A schematic diagram of the 3D view of the DOP (depth of penetration) test configuration is shown in **Figure 2g**. The ballistic test was positioned in such a way that the projectile first collided with the FGL and was fixed with a steel support profile to prevent vibration during the tests.

Ballistic setup was performed using the setup shown in **Figure 3**. The projectiles were fired from a rifled gun at a distance of 7.5 m. The projectile firing angle is perpendicular to the target. The velocity of the projectiles was measured using infrared light emitting diode-photovoltaic sensors and was approximately 715 m/s. In the experimental ballistic tests, 7.62 × 39 mm MSC-type ammunition was employed.

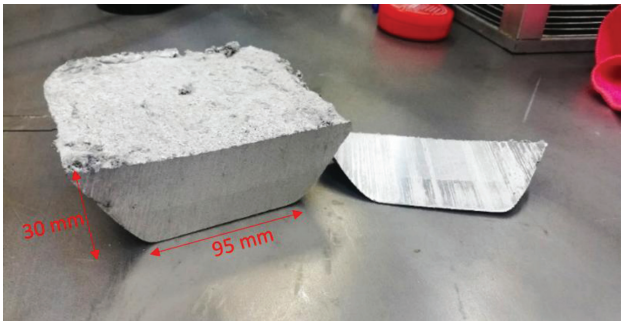

Figure 4: Ingots Produced by sedimentation Method

3 RESULTS

3.1 Characterization of Ingots

Figure 4 shows an ingot produced for ballistic tests and a cross-sectional image obtained by cutting through. Macropore formation was not observed in all of the produced casting ingots. When the cross-sectional image is examined, the layer formed as a result of sedimentation seen in dark color in the lower region draws attention.

In **Figure 5**, SEM images of the produced composites taken from the dark (A and B) and light (C) layers are presented. In the SEM images, it was observed that spherical white TiB_2 particles in regions A and B were homogeneously dispersed in the dark gray aluminum matrix. The size of the TiB_2 particles was determined to be around 2 micrometers. In contrast, no TiB_2 particles were observed in layer C. When the SEM images of layers A and B are compared, it is seen that the TiB_2 density is higher in layer A. This result showed that TiB_2 particles were functionally graded at different TiB_2 ratios from the bottom to the top of the casting ingots, forming a layer.

The results obtained show that TiB_2 particles are synthesized in-situ in liquid aluminum and then form a functionally graded layer (FGL) at the bottom of the ingot of the casting by sedimentation, as reported in previous studies. As a result of this process, ingots with function-

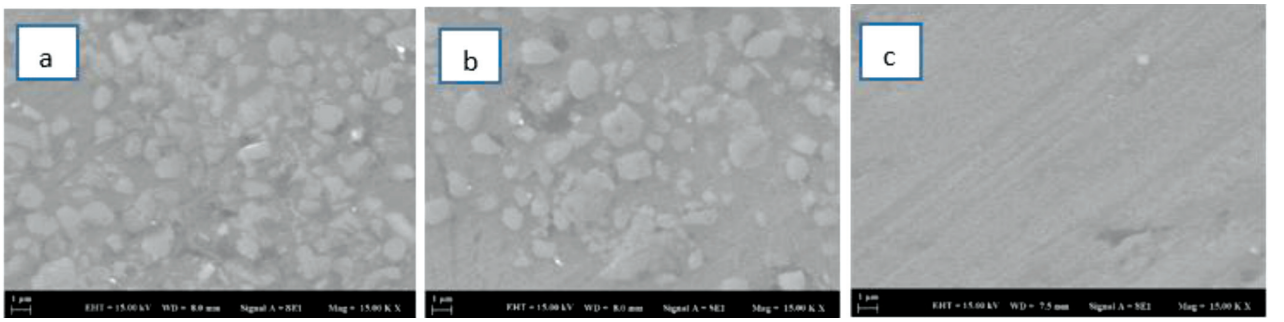

Figure 5: a) Layer C, b) Layer B, c) Layer A

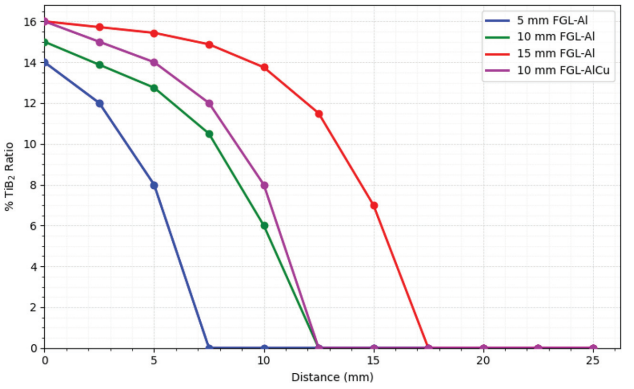

Figure 6: TiB_2 ratio based on Distance (φ/%

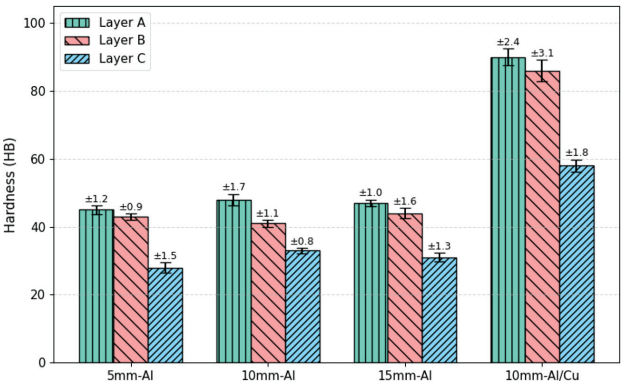

Figure 8: Macro hardness results of specimens

ally graded layers of (5, 10 and 15) mm thickness were successfully produced.

The volumetric reinforcement percentage of the ingots was calculated using the density values measured. For this calculation, the mixing rule equation given in Equation (1) was applied. The mixing rule is a fundamental approach used to determine the relationship between the densities and volumetric ratios of the matrix and reinforcement phases in composite materials.

$$\rho_c = V_f \cdot \rho_f + V_m \cdot \rho_m \quad (1)$$

In **Figure 6**, layered TiB_2 reinforcement ratio changes of 4 different ingots produced are presented. It is observed that TiB_2 reinforcement rates decrease from the bottom to the top of each ingot. According to the data obtained, the TiB_2 reinforcement ratio at the bottom of each ingot is around 15% and decreases functionally towards the top of the ingot. TiB_2 reinforcement ratio decreases to zero after (5, 10 and 15) mm distance. The probable reason for this situation is the precipitation of TiB_2 particles in liquid aluminum due to the density difference. Due to the sedimentation effect, heavy TiB_2 particles accumulate in the lower part of the casting, while layers with a lower reinforcement ratio are formed in the upper parts.

Based on the volumetric percent TiB_2 values, the theoretical modulus of elasticity of the cast ingots was calculated using the Halpin-Tsai model. As a result of the calculations, it was determined that the modulus of elasticity in the C layer without reinforcement was 70 GPa on average. On the other hand, it was determined that this value increased to approximately 95 GPa in A layers containing 15 *w*/% TiB_2 (**Figure 7**). No significant change in the elastic modulus of the Non-FGL – (Al-Cu) ingot was recorded. It has been reported by many researchers that increasing TiB_2 content causes an increase in elastic modulus.[23,24,25]

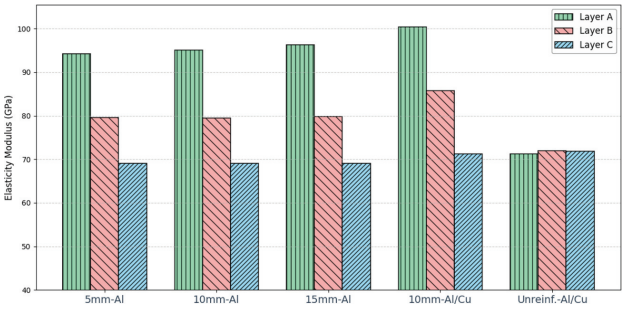

Figure 7: Elasticity Modulus of Composite Layers

In **Figure 8**, the average hardness values measured from TiB_2-reinforced layers A and B and unreinforced (C) layer of cast ingots with (5, 10 and 15) mm FGLs are presented. While the hardness value increased from an average of 57 HB in the layer C to an average of 90 HB for layer A of 10 mm FGL – (Al-Cu) ingot, the average hardness value was determined as 45 HB in layer A containing approximately 15% TiB_2 and 30 HB in layer C without TiB_2 for Al Ingots. In general, it has been observed that the hardness increases as the amount of TiB_2 particles added to Al increases.[26,27]

3.2 Depth of Penetration Test Results

Ballistic shooting results will enable observation of the effect of FGL thickness on ballistic performance. Projectiles that pass or partially pass through the armor samples will continue to penetrate towards the backing plate. Therefore, depending on the mechanical properties and ballistic performance of the armor sample, the progress of the projectile in the back plate varies. The less the depth of bullet penetration in the back plate, the better the efficiency and performance of the ballistic sample. Based on this assessment, the DOP (Depth of Penetration) test was performed. The ballistic performance of Al and Al-Cu ingots with different FGL thicknesses was investigated and the effect of FGL was analyzed.

Figure 9a shows that in the Al-Cu ingot containing 10 mm FGL, the projectile could not penetrate the armor specimen completely and the tip was damaged and bent. In **Figure 9b**, it is clearly observed from the yellow line that the projectile in the Al ingot containing 15 mm FGL cannot completely penetrate the armor sample, but penetrates more than the Al-Cu armor material containing

Table 2: DOP Test Result

Specimen	t (mm)	φ/% TiB_2		Bullet Velocity (m/s)	P_r (mm)	P_0 (mm)	DEF
		Layer A	Layer B				
5mm-FGL-Al	5	12.86	9.50	728.40	22.86	35.56	0.5
10mm-FGL-Al	10	13.87	9.380	727.80	19.04	35.56	0.64
15mm-FGL-Al	15	15.44	10.94	732.10	18.40	35.56	0.66
10mm-FGL-(Al-Cu)	10	15.20	10.80	731.20	12.13	35.56	0.88
Non-FGL-(Al-Cu)	0	0	0	727.80	Inefficent	35.56	0
Backing Plate	0	0	0	731.60	35.56	35.56	0

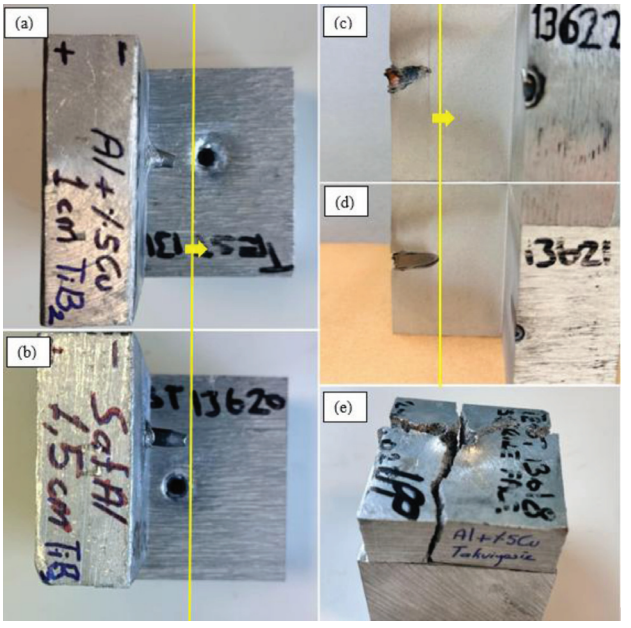

Figure 9: (a)10mm FGL – (Al-Cu) numune ve backing plate (b)15mm FGL – Al numune ve backing plate (c)10mm FGL – Al numunenin şahit plakası (d) 5mm FGL – Al numunenin şahit plakalası (e) Non-FGL – (Al-Cu) Ingot and Backing Plate

10 mm FGL. Since the Al armor specimen with 10 mm FGL in **Figure 9c** and the Al armor specimens with 5 mm FGL in **Figure 9d** were perforated, the penetration of the projectile was measured by cutting the backing plates of both specimens by wire erosion machine. As observed from the yellow line through their cross sections, the penetration increased in the Al armor specimen containing 5 mm FGL.

In **Figure 9e**, post-firing images of the Non-FGL – (Al-Cu) ingot are presented. As can be seen, the Non-FGL- (Al-Cu) completely disintegrated as a result of the ballistic impact, while the Al (**Figure 9a**) armor specimen containing 10 mm FGL maintained its structural integrity. This is related to the fact that the ballistic performance of composite armor is explained by specific impact mechanisms. In the layered composite armor model, the impact surface consists of a reinforced/strengthened layer, while the support/backing layer consists of a more ductile material with relatively lower stiffness. While the layer facing the projectile reduces the energy of the projectile instantaneously with the impact effect, the back layer, which exhibits tough and ductile properties, absorbs the energy of the projectile and stops it or further reduces its speed.[28]

The FGL reduces the kinetic energy of the projectile at the moment of contact, causing damage to the tip of the projectile. In this first stage, the kinetic energy undergoes a certain distribution and sudden drop. In the second stage, the unreinforced layer, which is more ductile than the FGL and has lower hardness, absorbs the kinetic energy and causes the projectile to stop or slow down. However, Non-FGL – (Al-Cu) does not have a functionally graded layer. In addition, the addition of copper increased the hardness of the Al-Cu alloy, while at the same time increasing its brittleness. As a result, the ductility of the back layer was insufficient for a projectile that did not experience a decrease in velocity and did not hit an FGL surface with high hardness. Therefore, it could not provide the desired ductility and sufficient toughness to stop the projectile. As a result, the Non-FGL - (Al-Cu) exhibited a brittle behavior and completely disintegrated when it encountered a projectile with a higher kinetic energy compared to the others.

In **Table 3**, the results of the DOP tests are presented. It was observed that the depth of penetration decreased with increasing FGL thickness. As shown in **Table 3**, penetration depths of 22.86 mm, 19.04 mm and 18.40 mm were obtained for samples with 5 mm, 10 mm and 15 mm FGL thicknesses, respectively. The best ballistic performance was measured in the Al-Cu ingot with 10 mm FGL and the penetration depth of this sample

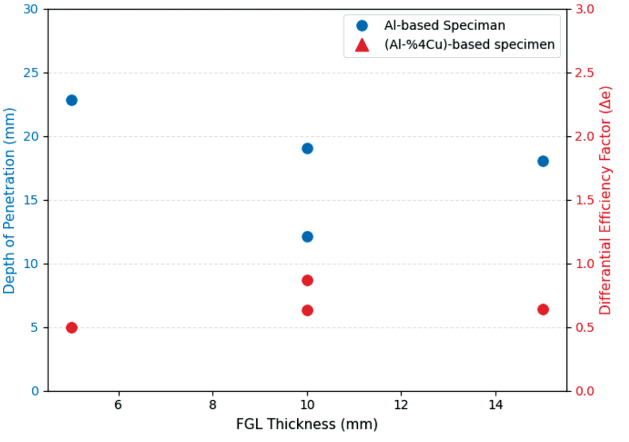

Figure 10: Ballistic Efficiency, DEF vs FGL Thickness

was 10.13 mm. The non-FGL (Al-Cu) ingot was deemed a failure as it disintegrated after the test.

The ballistic efficiency of the armor specimen was calculated using the Differential Efficiency Factor (DEF), in accordance with Equation (2).[29,30] The average reference penetration value (P_0) was obtained from tests conducted on a bare backing plate, while the Depth of Penetration (P_r) was determined for armor specimen placed in front of the same backing material.

$$DEF = \frac{\rho_b \times (P_0 - P_r)}{\rho_{FGL} \times t} \quad (2)$$

It is seen in **Figure 10** that the thickness of the functional graded layer (FGL) obtained by reinforcing with TiB_2 has a positive effects on ballistic performance. Increasing the FGL thickness caused the projectile impacting the ingot to encounter more resistance, reducing the penetration depth. The thickness of the FGL increases, it is observed that the average depth of penetration (DOP) decreases. When the FGL thickness reaches 15 mm for Al ingots without Cu, the penetration depth in the back plate decreases from 35.56 mm reference penetration to 18 mm. Therefore, as expected, it is clear that the ballistic performance of the armor specimens depends on the FGL thickness. It is also clearly seen that the optimum FGL thickness for the maximum DEF value can be 10 mm. The lowest penetration value was observed to be 12.13 mm in the 10 mm FGL - (Al-Cu) armor specimen.

The literature reports that functionally graded and layered armor structures exhibit superior ballistic performance compared to monolithic targets. In particular, it is stated that layers with high hardness and brittleness at the impact face rapidly reduce the projectile's penetration energy during the initial interaction, while the ductile and tough metallic phase at the rear region absorbs the remaining energy, thereby reducing the residual penetration depth.[31] Zhang[32] and Chao[33] demonstrated in their studies that, in functionally graded composites with different volumetric ceramic contents, the layer architecture directly influences ballistic performance, and that an optimized gradient distribution can achieve the same penetration resistance while reducing areal density. In addition, Li Jinzhu and colleagues showed that increasing the ceramic layer thickness leads to a reduction in residual penetration depth; however, this effect may vary depending on layer geometry and overall system optimization.[34] In this context, the literature demonstrates that ballistic performance is strongly dependent not only on material selection but also on layer architecture and thickness optimization. In addition, it has been determined that the Al-Cu matrix system used in this study, together with TiB_2 reinforcement, significantly enhances hardness and elastic modulus; the addition of Cu increases the load-bearing capacity of the matrix phase, resulting in a more rigid structure under impact conditions and thereby providing an indirect contribution to ballistic performance. The findings of this study similarly indicate that, in the functionally graded composite structure produced via in-situ synthesis and sedimentation, layer thickness is a critical parameter influencing ballistic performance; in particular, the observed decrease in ballistic efficiency for FGM layer thicknesses exceeding 10 mm reveals that armor design requires the simultaneous optimization of not only layered architecture, but also optimal thickness, gradient distribution, and alloying additions (such as Cu).

4 CONCLUSION

TiB_2 particle was synthesized in-situ in the aluminum matrix and sedimentation process was applied and 4 armor samples, Al ingot containing 5-10-15 mm functional graded layer (FGL), Al-Cu ingot containing 10 mm functional graded layer (FGL) and Non-FGL - (Al-Cu) ingot were successfully produced.

Increasing the reinforcement thickness of the Al armor specimen ingots to (5, 10 and 15) mm increased the ballistic efficiency and the penetration depth decreases to 22.86 mm-19.04 mm-18.40 mm, respectively.

The elastic modulus values increased in TiB_2 reinforced layers. In Al-Cu ingot containing 10 mm FGL, the elastic modulus was calculated as 96.96 GPa in layer A and 71.29 GPa in layer C.

The addition of 4 % Cu to Al ingot containing 10 mm FGL reduced the penetration depth from about 35 mm to 12.13 mm and increased the ballistic efficiency factor to over 0.88.

The Al-Cu armor sample containing 10 mm FGL gave the best results, while the Non FGL - (Al-Cu) ingot disintegrated as a result of the shot. This reveals the effect of FGL on ballistic protection.

It was determined that TiB_2-reinforced FGL thickness improved ballistic performance and Cu addition further enhanced this effectiveness, but copper alone was insufficient to increase ballistic resistance.

Nomenclature

FGL	Functionally Graded Layer
DOP	Depth of Penetration
V_m	Volume fraction of the matrix material (Al, Al-Cu, etc…)
V_f	Volume fraction of the reinforcement material (TiB_2, etc…)
ρ_f	Dencity of the reinforcement material
ρ_c	Density of the composite material
ρ_m	Density of the matrix material
ρ_b	Density of the backing plate material
ρ_{FGL}	Density of the FGL
P_0	Reference DOP in the backing plate
P_r	Residual DOP in the backing plate
t	Thickness of the FGL

Acknowledgments

The authors declare no conflict of interest, and their contributions are as follows: Author Ömer SAVAŞ and Ömer Faruk DEMİROK conceptualized the study, Author Muhammed Soner BAŞER conducted the necessary experimental work, analyzed the data, and wrote the manuscript. All authors contributed to revisions and approved the final version.

5 REFERENCES

[1] N. Kumar, G. Gautam, R. K. Gautam, A. Mohan, and S. Mohan, Synthesis and Characterization of TiB2 Reinforced Aluminium Matrix Composites: A Review, Journal of The Institution of Engineers (India) Series D, vol. 97, no. 2, pp. 233–253, Oct. 2015, doi:10.1007/S40033-015-0091-7

[2] S. Kumar, M. Chakraborty, V. Subramanya Sarma, and B. S. Murty, Tensile and wear behaviour of in situ Al-7Si/TiB2 particulate composites, Wear, vol. 265, no. 1–2, pp. 134–142, Jun. 2008, doi:10.1016/J.WEAR.2007.09.007

[3] Y. Shen, X. Li, T. Hong, J. Geng, and H. Wang, Effects of TiB2 particles on microstructure and mechanical properties of an in-situ TiB2-Al-Cu-Li matrix composite, Materials Science and Engineering: A, vol. 655, pp. 265–268, Feb. 2016, doi:10.1016/J.MSEA.2015.12.104

[4] G. Geandier, S. Denis, A. Hazotte, and A. Mocellin, Hertzian crack analysis in alumina–chromium composites, J. Eur. Ceram. Soc., vol. 25, no. 7, pp. 1119–1132, May 2005, doi:10.1016/J.JEURCERAMSOC.2004.04.022

[5] K. Niranjan and P. R. Lakshminarayanan, Dry sliding wear behaviour of in situ Al–TiB2 composites, Mater. Des., vol. 47, pp. 167–173, May 2013, doi:10.1016/J.MATDES.2012.11.035

[6] H. B. Michael Rajan, S. Ramabalan, I. Dinaharan, and S. J. Vijay, Synthesis and characterization of in situ formed titanium diboride particulate reinforced AA7075 aluminum alloy cast composites, Materials & Design (1980-2015), vol. 44, pp. 438–445, Feb. 2013, doi:10.1016/J.MATDES.2012.08.008

[7] E. Kocaman, B. Kılınç, Ş. Şen, and U. Şen, Development of Surface Properties with In Situ TiB2 Intermetallic-Assisted Coating by Fe(18-X)Ti2BX (x?=?3,4,5)-Based Electrodes, Arabian Journal for Science and Engineering 2021 47:7, vol. 47, no. 7, pp. 8485–8501, Nov. 2021, doi:10.1007/S13369-021-06304-0

[8] W. Wang, Z. Fu, H. Wang, and R. Yuan, Influence of hot pressing sintering temperature and time on microstructure and mechanical properties of TiB2 ceramics, J. Eur. Ceram. Soc., vol. 22, no. 7, pp. 1045–1049, Jul. 2002, doi:10.1016/S0955-2219(01)00424-1

[9] A. Pettersson, P. Magnusson, P. Lundberg, and M. Nygren, Titanium–titanium diboride composites as part of a gradient armour material, Int. J. Impact Eng., vol. 32, no. 1–4, pp. 387–399, Dec. 2005, doi:10.1016/J.IJIMPENG.2005.04.003

[10] E. Balcı, B. Sarıkan, M. Übeyli, N. Camuşcu, and R. O. Yıldırım, On the ballistic performance of the AA7075 based functionally graded material with boron carbide reinforcement, Kovove Materialy, vol. 51, no. 4, pp. 257–262, Jan. 2013, doi:10.4149/KM_2013_4_257

[11] M. Übeyli et al., The ballistic performance of SiC-AA7075 functionally graded composite produced by powder metallurgy, Mater. Des., vol. 56, pp. 31–36, 2014, doi:10.1016/J.MATDES.2013.10.092

[12] J. J. Sobczak, L. Drenchev, and R. Asthana, Nomograms for rapid assessment of particle sedimentation behaviour in liquid phase processing of particle reinforced metal composites, International Journal of Cast Metals Research, vol. 26, no. 2, pp. 122–128, Apr. 2013, doi:10.1179/1743133612Y.0000000045

[13] B. Previtali, D. Pocci, and C. Taccardo, Application of traditional investment casting process to aluminium matrix composites, Compos. Part A Appl. Sci. Manuf., vol. 39, no. 10, pp. 1606–1617, Oct. 2008, doi:10.1016/J.COMPOSITESA.2008.07.001

[14] E. Kocaman, B. Kılınç, Ş. Şen, and U. Şen, In-situ TiB2 and Fe2Ti intermetallic assisted hard coatings by Fe-Ti-B based hardfacing electrodes, J. Alloys Compd., vol. 900, p. 163478, Apr. 2022, doi:10.1016/J.JALLCOM.2021.163478

[15] S. Ren, X. He, X. Qu, and Y. Li, Effect of controlled interfacial reaction on the microstructure and properties of the SiCp/Al composites prepared by pressureless infiltration, J. Alloys Compd., vol. 455, no. 1–2, pp. 424–431, May 2008, doi:10.1016/J.JALLCOM.2007.01.127

[16] S. Kumar, M. Chakraborty, V. Subramanya Sarma, and B. S. Murty, Tensile and wear behaviour of in situ Al–7Si/TiB2 particulate composites, Wear, vol. 265, no. 1–2, pp. 134–142, Jun. 2008, doi:10.1016/J.WEAR.2007.09.007

[17] C. S. Ramesh, S. Pramod, and R. Keshavamurthy, A study on microstructure and mechanical properties of Al 6061-TiB2 in-situ composites, Materials Science and Engineering: A, vol. 528, no. 12, pp. 4125–4132, 2011, doi:10.1016/J.MSEA.2011.02.024

[18] E. Kocaman, H. Aydın, K. Yiğit, F. Çalışkan, and Ö. Savaş, Corrosion Behaviour of Al/(TiB2?+?-Al3Ti)-Based Functional Grade Metal Matrix Composite by Sedimentation Method, Transactions of the Indian Institute of Metals 2024 77:8, vol. 77, no. 8, pp. 2153–2161, Apr. 2024, doi:10.1007/S12666-024-03301-3

[19] U. Akyol, E. Kocaman, Ö. Savaş, SEDİMANTASYON YÖNTEMİ İLE FONKSİYONEL DERECELENDİRİLMİŞ TİB2/AL-CU-Sİ KOMPOZİTLERİN ÜRETİLE BİLİRLİĞİNİN ARAŞTIRILMASI, Accessed: Jun. 13, 2025. [Online]. Available: https://avesis.yildiz.edu.tr/yayin/4633d03d-a74a-4815-99ec-3ff98839801d/sedimantasyon-yontemi-ile-fonksiyonel-derecelendirilmis-tib2-al-cu-si-kompozitlerin-uretile-bilirliginin-arastirilmasi

[20] M. Gokelma, G. Gokelma, K. E. Einarsrud, G. Tranell, and B. Friedrich, Shape Factor Effect on Inclusion Sedimentation in Aluminum Melts, doi:10.1007/s11663-020-01769-0

[21] S. G. Shabestari and J. E. Gruzleski, Gravity segregation of complex intermetallic compounds in liquid aluminum-silicon alloys, Metallurgical and Materials Transactions A 1995 26:4, vol. 26, no. 4, pp. 999–1006, Apr. 1995, doi:10.1007/BF02649097

[22] E. T. Y. Yildiz, Ö. Savaş, M. S. Başer, and E. Kocaman, Abrasive wear behavior of functionally graded Al3Ti reinforced aluminum matrix composite, SpringerETY Yildiz, Ö Savaş, MS Başer, E KocamanChina Foundry, 2025Springer, vol. 22, no. 1, Jan. 2024, doi:10.1007/S41230-024-3147-1

[23] Z. Lv, J. Sha, G. Lin, J. Wang, Y. Guo, and S. Dong, Mechanical and thermal expansion behavior of hybrid aluminum matrix composites reinforced with SiC particles and short carbon fibers, J. Alloys Compd., vol. 947, Jun. 2023, doi:10.1016/J.JALLCOM.2023.169550

[24] T. V. Christy, N. Murugan, and S. Kumar, A Comparative Study on the Microstructures and Mechanical Properties of Al 6061 Alloy and the MMC Al 6061/TiB<sub>2</ sub>/12_p, Journal of Minerals and Materials Characterization and Engineering, vol. 09, no. 01, pp. 57–65, 2010, doi:10.4236/JMMCE.2010.91005

[25] Q. Song, X. Du, W. Dong, H. Liang, H. Shi, and J. Liu, Study on the dynamic compression properties of a 0.5 % Graphene/6061 aluminum matrix composite, Materials and Technology, vol. 59, no. 5, pp. 675-682–675–682, Sep. 2025, doi:10.17222/MIT.2025.1428

[26] A. Gavel, S. Poria, and P. Sahoo, Design of experiments analysis of abrasive friction behavior of Al-TiB2 composites, Mater. Today Proc., vol. 19, pp. 218–222, 2019, doi:10.1016/J.MATPR.2019.06.705

[27] Ö. Savaş, Fabrication and characterization of TiB2-reinforced functionally graded aluminum matrix material, Industrial Lubrication and Tribology, vol. 72, no. 10, pp. 1147–1152, Nov. 2020, doi:10.1108/ILT-12-2019-0538/

[28] S. Sadanandan and J. G. Hetherington, Characterisation of ceramic/steel and ceramic/aluminium armours subjected to oblique impact, Int. J. Impact Eng., vol. 19, no. 9–10, pp. 811–819, Oct. 1997, doi:10.1016/S0734-743X(97)00019-5

[29] S. G. Savio and V. Madhu, Effect of Tile Thickness and Projectile Velocity on the Ballistic Performance of Boron Carbide Against 12.7 mm AP, Procedia Eng., vol. 173, pp. 286–292, Jan. 2017, doi:10.1016/J.PROENG.2016.12.015

[30] Z. Rozenberg and Y. Yeshurun, The relation between ballastic efficiency and compressive strength of ceramic tiles, Int. J. Impact Eng., vol. 7, no. 3, pp. 357–362, Jan. 1988, doi:10.1016/0734-743X(88)90035-8

[31] J. Wu, Z. Qin, L. Qu, H. Zhang, F. Deng, and M. Guo, Natural hydrogel in American lobster: A soft armor with high toughness and strength, Acta Biomater., vol. 88, pp. 102–110, Apr. 2019, doi:10.1016/J.ACTBIO.2019.01.067

[32] R. wei Zhang et al., Ballistic performance and mechanism of B_4C/Al laminated targets with different configurations, Journal of Materials Research and Technology, vol. 27, pp. 7807–7822, Nov. 2023, doi:10.1016/j.jmrt.2023.11.227

[33] Z. L. Chao et al., The microstructure and ballistic performance of B_4C/AA2024 functionally graded composites with wide range B_4C volume fraction, Compos. B Eng., vol. 161, pp. 627–638, Mar. 2019, doi:10.1016/J.COMPOSITESB.2018.12.147

[34] L. Jinzhu, Z. Liansheng, and H. Fenglei, Experiments and simulations of tungsten alloy rods penetrating into alumina ceramic/603 armor steel composite targets, Int. J. Impact Eng., vol. 101, pp. 1–8, Mar. 2017, doi:10.1016/j.ijimpeng.2016.09.009